Evolution of Envelope Sequences of Human Immunodeficiency Virus Type 1 in Cellular Reservoirs in the Setting of Potent Antiviral Therapy

HULDRYCH F. GÜNTHARD,[1]† SIMON D. W. FROST,[2] ANDREW J. LEIGH-BROWN,[2]
CAROLINE C. IGNACIO,[1] KRISTIN KEE,[1] ALAN S. PERELSON,[3] CELSA A. SPINA,[1,4]
DIANE V. HAVLIR,[1] MARJAN HEZAREH,[1] DAVID J. LOONEY,[1,4]
DOUGLAS D. RICHMAN,[1,4] AND JOSEPH K. WONG[1,4]*

University of California, San Diego,[1] *and San Diego Veterans Affairs Healthcare System,*[4]
San Diego, California; University of Edinburgh, Edinburgh, Scotland[2]*; and
the Los Alamos National Laboratory, Los Alamos, New Mexico*[3]

In human immunodeficiency virus (HIV)-infected patients treated with potent antiretroviral therapy, the persistence of latently infected cells may reflect the long decay half-life of this cellular reservoir or ongoing viral replication at low levels with continuous replenishment of the population or both. To address these possibilities, sequences encompassing the C2 and V3 domains of HIV-1 *env* were analyzed from virus present in baseline plasma and from viral isolates obtained after 2 years of suppressive therapy in six patients. The presence of sequence changes consistent with evolution was demonstrated for three subjects and correlated with less complete suppression of viral replication, as indicated by the rapidity of the initial virus load decline or the intermittent reappearance of even low levels of detectable viremia. Together, these results provide evidence for ongoing replication. In the remaining three patients, virus recovered after 2 years of therapy was either genotypically contemporary with or ancestral to virus present in plasma 2 years before, indicating that virus recovery had indeed resulted from activation of latently infected cells.

Treatment with combination antiretroviral agents can reduce plasma and lymph node RNA levels below the level of detection of sensitive assays for nucleic acid (2, 12, 31, 46). The persistence of cells harboring replication-competent virus despite periods of up to 3 years of potent suppressive therapy has raised questions about the feasibility of eradication of infection with currently recommended treatments (3, 9, 10, 47, 49). Despite the apparent lack of development of drug resistance in patients with undetectable virus (9, 47), the inferred presence of unintegrated viral DNA in peripheral blood mononuclear cells (PBMC) in one study (3) has raised questions about the certainty that viral replication is controlled even in this setting. Extrapolating from such observations, it can be argued that the persistence of this reservoir of virus reflects ongoing viral replication at low levels and continuous replenishment rather than the existence of long-lived, latently infected cells.

To address this question, we studied sequences of the human immunodeficiency virus type 1 (HIV-1) envelope corresponding to the relatively conserved C2 and the hypervariable V3 domains of *env* from HIV-1 present in baseline plasma and in virus recovered from in vitro culture of PBMC following 2 years of therapy. The V3 region is an important determinant of cell tropism and is a target of host immune responses. Consequently, it is among the most variable regions in the HIV genome (15, 19, 21, 36). Sequence differences in this region have been used to compare the relatedness of virus populations (20, 33, 42) and to study viral evolution within individual hosts (1a, 6, 37–39, 45), among patients (1a, 6, 25, 26, 37, 38, 45), and across patient populations (21, 22, 27).

Samples were studied from six individuals from whom, despite prolonged suppression of plasma viremia, virus had been previously recovered by coculture of PBMC (47). We hypothesized that ongoing replication should be accompanied by changes in viral envelope sequence and that phylogenetic analysis would permit the distinction of virus produced by activation of latently infected cells from that produced as a consequence of continued viral propagation during the course of therapy.

(Presented in part at the 2nd International Workshop on HIV Drug Resistance and Treatment Strategies, Lake Maggiore, Italy, June 1998.)

MATERIALS AND METHODS

Patient selection. Subjects were chosen from a well-characterized cohort of HIV-infected patients undergoing treatment with indinavir, lamivudine, and zidovudine (12, 47). Each had apparent suppression of plasma and serum viral RNA to below the 50-copy/ml level with the exception of patient M, who had 50 copies of HIV RNA/ml on the day of PBMC sampling for virus isolation (Fig. 1). Sequence comparisons were made between virus present in baseline plasma and virus isolated while on drug therapy at year 2.

Viral isolates. The materials and methods for viral isolation have been previously published (47). Early culture supernatants were chosen to minimize ex vivo culture effects on the composition of the viral isolates (typically at day 14 of original cultures and before peak p24 production).

RNA extraction. RNA was extracted from cell-free viral culture supernatants with the Qiagen HCV RNA extraction kit (Qiagen, Chatsworth, Calif.) and from plasma by the AMPLICOR extraction procedure (Roche Diagnostics, Branchburg, N.J.) according to the manufacturers' protocols.

RT-PCR. Following denaturation of the RNA template and primer mix at 70°C for 3 min, reverse transcription (RT) was performed at 45°C for 1 h in the following buffer: 100 mM Tris (pH 8.3), 10 mM MgCl, 50 mM KCl, 10 mM dithiothreitol, 250 µM dinucleoside triphosphate, 37 U of RNAgard (Pharmacia), 2.5 U of avian myeloblastosis virus reverse transcriptase (Gibco BRL, Gaithersburg, Md.), 12.5 pmol of V3Bout primer (5′-ATTACAGTAGAAAAA TTCCCCT-3′). Nested PCRs were then performed in quadruplicate for each

* Corresponding author. Mailing address: Stein Clinical Research Building No. 326, University of California, San Diego, 9500 Gilman Dr., La Jolla, CA 92093-0679. Phone: (619) 552-8585, ext. 7193. Fax: (619) 552-7445. E-mail: j2wong@ucsd.edu.
† Present address: University of Zürich, Zürich, Switzerland.

Serial RNA group 1

Serial RNA group 2

Serial RNA group 3
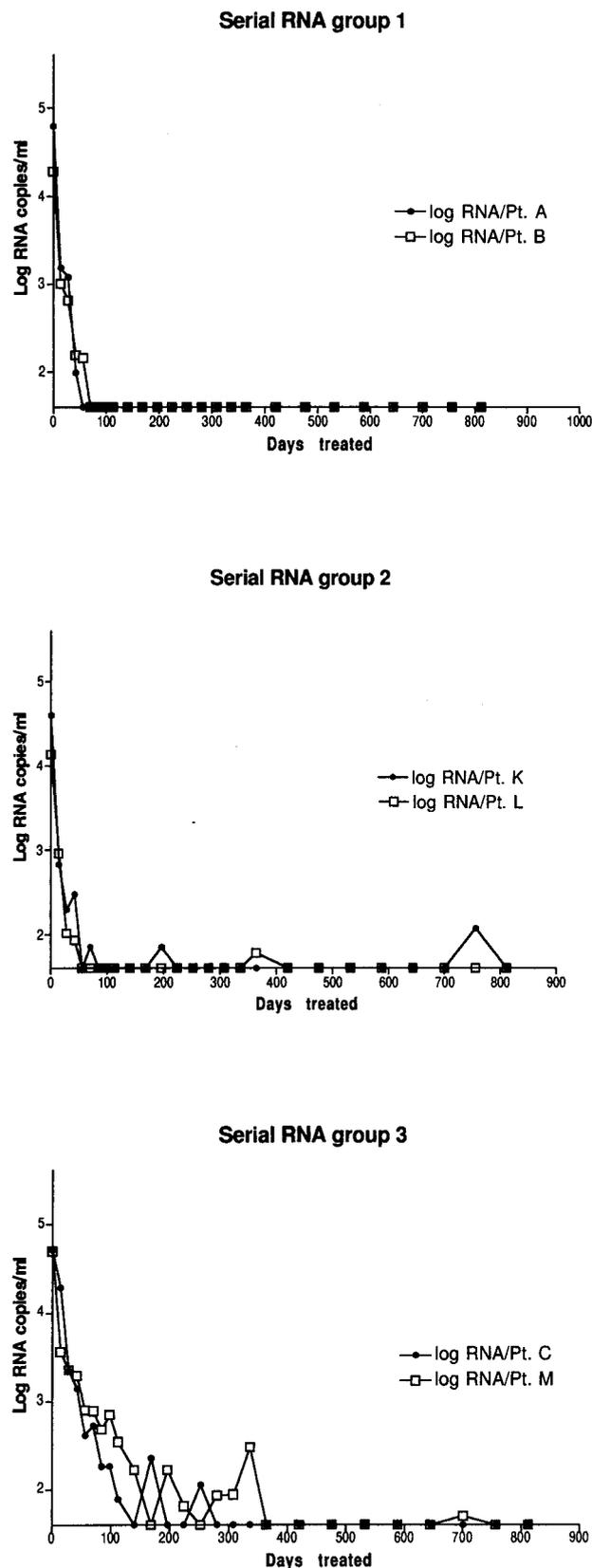
FIG. 1. Log RNA copies/ml in serum or plasma plotted against days under indinavir, zidovudine, and lamivudine combination therapy. The baseline for the *y* axis is the limit of detection of the Roche ultrasensitive assay (1.6 log copies/ml). The top panel demonstrates the response of two patients (Pt.) with steep

sample to minimize sampling bias. RT product (cDNA; 10 μl) was carried over to a first-step PCR employing the primers V3Bout and V3Fout (5'-CAAAGG TATCCTTTGAGCCAAT-3') under the following reaction and thermocycling conditions: Tris (pH 8.3), 3 mM MgCl$_2$, 250 μM deoxynucleoside triphosphate, 20 pmol of primers, 1 mg of bovine serum albumin/ml, 5 U of *Taq* polymerase (Boehringer Mannheim) in a 50-μl reaction volume at 95°C for 2 min, 95°C for 30 s, 55°C for 30 s, 72°C for 1 min for 35 cycles; and 72°C for 1 min. One microliter of the first-step product was then carried over to a second-step PCR with the primers V3Fin (5'-GAACAGGACCAGGATCCAATGTCAGCACAG TACAAT-3') and V3Bin (5'-GCGTTAAAGCTTCTGGGTCCCCTCCTGAG-3') with reaction conditions identical to those for the first-step PCR. Ten percent of the PCR products were resolved on 1% agarose gels and visualized by ethidium bromide staining. We have examined the rate of misincorporation during amplification under these nested PCR conditions by comparing the results from sequencing of unamplified pNL4-3 (1) with those from sequencing of amplified and subsequently cloned products and have observed a misincorporation frequency of approximately 1 to 3 per 3,500 bases.

Cloning. After determination that each of quadruplicate nested PCR products yielded comparable band intensities by ethidium staining, 5 μl of each of the quadruplicate reactions were pooled together and gel purified by agarose gel electrophoresis. DNA was extracted from gel slices with the Qiaex II Gel Extraction kit (Qiagen) according to the manufacturer's protocol. Two microliters of the pooled, gel-purified PCR products was ligated into the plasmid vector pCR 2.1 and cloned according to the instructions for the TOPO Ta Cloning system (Invitrogen, Carlsbad, Calif.) under ampicillin selection.

Sequencing. Ten to 13 individual clones were picked based on blue-white screening and grown in 3-ml cultures. Plasmids were purified with the Qiaprep Turbo-8 kit (Qiagen). Approximately 300 ng of each plasmid was sequenced with the sequencing primers ForTopoEcoR1 (5'-TGGATATCTGCAGAATTCG-3') and M13 Reverse (5'-CAGGAAACAGCTATGAC-3') with a 373A automated sequencer and Big-dye chain terminator chemistry (Applied Biosystems, Inc., Foster City, Calif.). The sequences were aligned and manually edited with Sequence Navigator 1.1 (Applied Biosystems). In total, 115 evaluable sequences were obtained for the six patients.

Phylogenetic analysis. Tree reconstructions were performed by a neighbor-joining method implemented with DNADIST (Kimura distances; transition transversion ratio, 2.0) and NEIGHBOR in Phylip version 3.54 (7) with 100 bootstrapped data sets and by a maximum-likelihood method with fastDNAML (7, 30), applying a transition/transversion ratio of 2.0 and a uniform substitution rate. Graphic representation of phylogenetic trees was accomplished with Treeview version 1.5 (30a).

Determination of pairwise distances. Pairwise distances from the most recent common ancestor (MRCA; represented by the most distal node which gives rise to all sequences from the same patient) to clonal sequences on the maximum-likelihood phylogenetic tree were estimated both by summing relevant branch lengths generated with fastDNAML version 1.0 (random input order; transition/transversion ratio, 2.0; single rate of substitution) (7, 30) and by direct computation with DNADIST (PHYLIP version 3.54; maximum-likelihood estimates; transition/transversion ratio, 2.0) (7) from the inferred MRCA sequences obtained with DNAML (PHYLIP version 3.6) (7, 8). Branch lengths from fastDNAML were chosen over those provided by DNAML (PHYLIP version 3.6) because the latter presently assigns a minimum distance of 0.00005 to every segment of inferred maximum-likelihood trees, including branches connecting identical sequences. However, the two programs produced trees with comparable maximum-likelihood values. Duplicate analyses were performed, with selection of the MRCA based on all viral isolate sequences and the nearest plasma sequences (changed the selection of the MRCA for patients A, C, and M). Means and standard errors for distances were calculated with JMP version 3.1.5 (SAS, Cary, N.C.).

Mean pairwise distances between plasma virus and viral isolates were calculated with the program SENDBS (Naoko Takeaki) with and without correcting for within-sample diversity (29).

Estimation of residual replication. Residual HIV replication was approximated by calculation of the area under the curve (AUC) generated by plotting log plasma RNA against time. The observed AUC (AUC$_{Obs}$) represented the log RNA copy by time product which results from the decay of free virus in plasma and virus produced by cells infected prior to institution of therapy (productively infected cells; a reservoir of "long-lived" infected cells; and release of virus from the follicular dendritic network in lymphoid tissues and activation of latently infected cells) as well as from any virus produced as a consequence of ongoing viral replication during combination therapy.

The theoretical AUC for each patient was estimated according to the long-lived-infected-cell model of Perelson et al. (31). This calculation assumes decay

initial declines in viral load (A and B). The middle panel shows two patients with steep initial declines followed by transient reappearance of low levels of detectable viral RNA (K and L). The bottom panel shows two patients with slow initial responses (C and M) and, in one patient (M), intermittent transient reappearance of low levels of viral RNA in the blood.

in the absence of residual viral replication under therapy and assumes that activation of latent cells contributes relatively little to the viral RNA measured during first- or second-phase decay of plasma virus. $\log_{10}$ viral RNA copy number ($\log_{10}V$) as a function of time (t) can be described as follows:

$$\log_{10}V(t) = \log_{10}V_0\Bigg([NkT_0/(c-\delta)]e^{-\delta t} + [(c-NkT_0)/(c-\mu_M)]e^{-\mu_M t} + \{1$$

$$- [NkT_0/(c-\delta)] - [(c-NkT_0)/(c-\mu_M)]\}e^{-ct}\Bigg) \qquad (1)$$

where V_0 is the viral load at baseline, δ is the decay constant of productively infected cells, μ_M is the decay constant of long-lived cells, c is the clearance constant for virions, T_0 is the CD4 count at baseline, N is the viral burst size, and k is the infection constant (31). Perelson et al. observed NkT_0 values between 2.84 and 2.92 for a T_0 of 205 to 500 cells/mm^3. We utilized a mean value for NkT_0 of 2.88 and the observed virus clearance constant, c, of 3 day^{-1} in our analysis (32).

The serially measured viral RNA concentrations and those calculated from equation (1) were plotted against time under treatment with the program PRISM 2.0 (Graphpad, San Diego, Calif.). AUCs were calculated by summation of trapezoids implemented in the program PRISM 2.0. The predicted AUC (AUC$_{Pred}$) was computed with a δ of 1.2 day^{-1} and a μ_M of 0.115, based on the best-case decay constants observed by Perelson et al. (31). Duplicate analyses with a δ of 0.7 day^{-1} and a μ_M of 0.066 based on mean decay constants (31) for the calculation of AUC$_{Pred}$ resulted in very similar results (data not shown). The difference between AUC$_{Obs}$ and AUC$_{Pred}$, then, represented the proportion of the RNA concentration by time product that should be attributable to residual viral replication for each patient while under therapy (AUC$_{Net}$).

In general, the use of AUC as an indicator of the difference in the degree of ongoing viral replication between patients may be best when their baseline RNA concentrations are similar, while the calculation of AUC$_{Net}$ from AUC$_{Obs}$ and AUC$_{Pred}$ becomes most necessary when baseline RNA concentrations vary greatly among the patients being compared. In the present study, the patients had similarly uniform starting RNA levels.

Our calculations assumed negligible contribution to total viremia from sporadic activation of latently infected cells (a simplification justified by observations of phase 1 and phase 2 decay by Perelson et al. [31]) and may therefore tend to underestimate the AUC$_{Pred}$, leading to overestimates of AUC$_{Net}$. Because of this and other assumptions made for the derivation of these terms, it would be incorrect to treat the calculated values as definitive for residual viral replication. Rather, they are meant to represent a relative magnitude of residual replication (derived from the best available kinetic data and based on prevailing theory in the published literature) and are applied here to permit reasonable interpatient comparison.

Statistical analyses. Correlations of AUC$_{Net}$ with pairwise genetic distance and Wilcoxon rank sums for comparison of pairwise distances were computed with the statistical analysis program JMP 3.1.5. (SAS) and the program Prism 2.0.

Nucleotide sequence accession numbers. All sequences reported here have been deposited in GenBank and were given accession no. AF185823 to AF185937.

RESULTS

Assessment of residual viral replication based on the response of serum and plasma RNA to drug therapy permitted segregation of the patients into three patterns (Fig. 1). Group 1 (patients A and B) had subjects with the steepest initial declines in viral load and without any detectable viral RNA for the duration of this study period. Group 2 patients (K and L) were subjects who had similarly rapid initial declines in plasma virus concentrations upon initiation of therapy but with sporadic reappearance of low but detectable levels of viremia later. Finally, two patients (C and M) constituted a third group exhibiting a protracted and gradual decline in plasma virus levels with later sporadic reappearance of viremia throughout the first 2 years of therapy. In the case of M, viral RNA was present in plasma at the same time that samples were obtained for viral culture (47). The amount of residual replication as reflected by AUC$_{Net}$ was low to negligible for patients A, B, and L, intermediate for K and C, and highest for patient M (Table 1).

Phylogenetic reconstruction. In every case, sequences from each patient clustered together and not with those from other patients or with prototypic laboratory-adapted and "primary" HIV clones, as shown by a reconstruction by maximum-likeli-

TABLE 1. Residual viral replication[a]

Patient	AUC$_{Obs}$	AUC$_{Pred}$	AUC$_{Net}$
A	70.74	43.90	26.84
B	71.49	27.24	44.25
L	54.81	24.13	30.68
K	97.60	36.81	60.79
C	194.3	40.97	153.33
M	276.1	40.47	235.63

[a] $\log_{10}$ RNA copies/ml $\times$ day products for each patient grouped according to pattern of RNA response following initiation of therapy (Fig. 1). The AUCs were calculated with a baseline equal to the threshold of sensitivity of the Roche ultrasensitive assay, 1.6 $\log_{10}$ RNA copies/ml. AUC$_{Obs}$ is the product obtained from the measured values plotted in Fig. 1. AUC$_{Pred}$ was calculated based on a mathematical model from Perelson et al. using the best-case decay constants observed by Perelson. AUC$_{Net}$ is the difference between AUC$_{Pred}$ and AUC$_{Obs}$ and represents the proportion of the AUC that may reflect ongoing viral replication and/or production of virus from activation of latent cells (see the text).

hood analysis (Fig. 2) (24). Tree topology with a neighbor-joining reconstruction was similar: sequences from each patient formed individual clusters with highly significant bootstrap values (>80 per 100 bootstrapped data sets examined) in the consensus neighbor-joining tree (data not shown). In one case (patient B), year 2 isolates were indistinguishable from sequences present at baseline and were very homogeneous. For patients A and C, the viral isolates most closely resembled one or a subset of sequences present in baseline plasma, while for patients K, L, and M, no plasma sequences were identified which clearly clustered with sequences from year 2 viral isolates, although in the case of M, a "nearest plasma clone" could be identified. For patients M and C, branch lengths from the closest proximal common node (representing the most recent common ancestor) to the year 2 isolates appeared longer than those to the baseline plasma sequences.

Protein sequence comparisons. In four patients, inferred protein sequences demonstrated little difference between baseline and year 2 isolates in the C2 region (Fig. 3). In the V3 region, baseline sequences differed from year 2 viral isolates at multiple positions in the case of patient M, while few differences were noted for the other five subjects. For patient M, an S-to-R substitution was seen at position 306 (according to HXB2 sequence by convention of the Los Alamos National Laboratories) in the V3 loop which has been associated with a switch from M- to T-cell tropism (4, 11), but cell tropism and presumably coreceptor usage are context dependent (40). In this patient there was an accompanying R-to-S replacement at residue 322. Cultivation of the year 2 virus in an MT-2 cell assay (34) showed that it was non-syncytium inducing (data not shown). In the case of patient K, multiple replacements were noted in the region downstream from the V3 loop, towards V4.

Pairwise genetic distances between baseline plasma virus and year 2 viral isolates. Pairwise genetic distances (both corrected and uncorrected for overall diversity of clones from each source) demonstrated a continuum of small but measurable distances between baseline plasma-derived sequences and 2-year viral isolates. Corrected distances demonstrated considerably greater variability than uncorrected ones due to substantial variation among patients in the level of diversity in plasma samples (Table 2). A more conservative calculation of net divergence was also made by using the diversity of the time zero plasma population as an estimate of the true diversity of virus in the population of viably infected cells at year 2. The rank orders of divergence in these analyses were similar, with M and K showing the greatest divergence (data not shown).
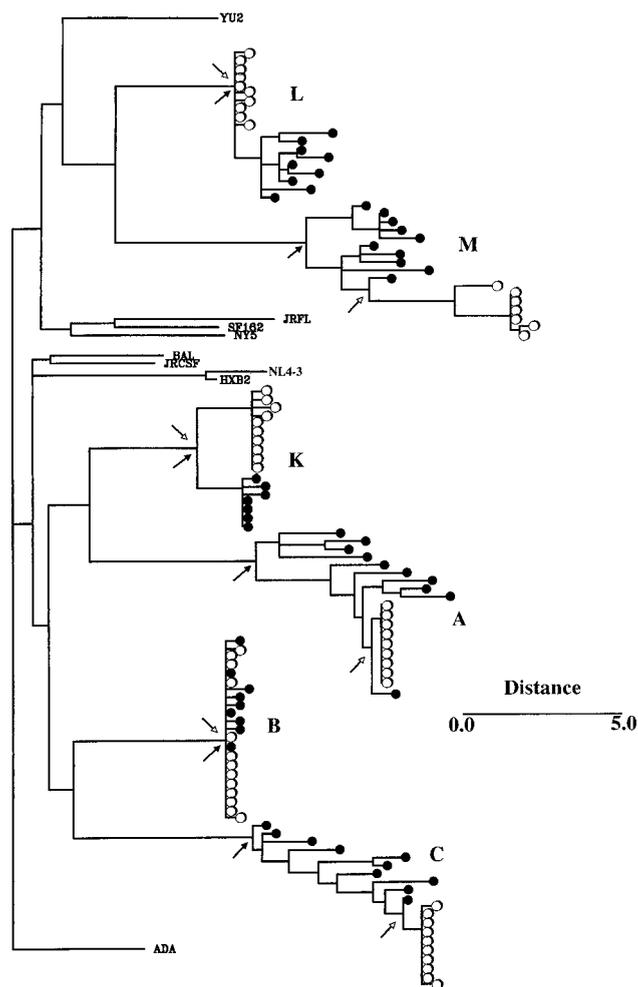
FIG. 2. Maximum-likelihood phylogenetic tree displaying relationships of sequences of clones derived from plasma collected at the start of therapy (time zero) and from viral isolates obtained approximately 2 years into therapy. The letters adjacent to individual sequence clusters identify the patient source of the sequences. In every case, the sequences from an individual patient clustered with sequences from the same patient and with no others. Sequences of prototypic T-lymphocytotrophic and macrophage-tropic viruses are denoted by the respective reference names (NL4-3, SF162, etc.). Sequences derived from baseline plasma are represented by solid circles. Sequences derived from viral isolates are indicated by open circles. The arrows with solid arrowheads identify nodes representing the MRCA identified for all plasma and viral isolate sequences from each patient. The arrows with open arrowheads identify nodes representing the MRCA for the viral isolate cluster and the plasma viral sequence(s) nearest it. Horizontal branch lengths are scaled and correspond approximately to the percent nucleotide differences between sequences and nodes. Sequences whose branch lengths were not significantly different from zero are shown with collapsed branches.

Genetic distance to MRCA. Based on coalescence theory (17, 18, 35, 41), each sequence can be traced back to the most recent common ancestral sequence (the MRCA, represented by the most distal node common to all sequences from each patient on the phylogenetic tree [Fig. 2]), with branch lengths proportional to the number of elapsed generations. Here we assume that the mutation rate μ is relatively constant among individuals so that sequence divergence is determined by gt, where g is the number of generations (replication cycles) times time^{-1} and t is the elapsed time. Although mutations within the reverse transcriptase have been reported to affect the fi-

delity of HIV-1 RT (43), such mutations were not observed in these viral isolates (47).

The difference between mean genetic distances from year 2 viral sequences and those from year zero plasma sequences to the MRCAs for each patient was calculated to provide a relative measure of generations elapsed since the common ancestor. Larger positive differences would be expected when year 2 isolates are more divergent from the MRCA than baseline plasma virus, and increasingly more negative values would be expected when the viral isolates are genealogically older than baseline plasma virus (Table 3). When MRCAs for each patient were identified based on all available sequences, the distances from the MRCA to year 2 viral isolates exceeded the distances from the MRCA to the baseline plasma sequences derived by summation of branch lengths for three patients (M [$P = 0.0006$ for Wilcoxon rank sum], C [$P = 0.001$], and K [$P = 0.0208$]), were equivalent for one (A [$P = 0.667$]) and were less for two (B [$P = 0.0023$] and L [$P = 0.0002$]) subjects. The results were qualitatively similar for distances generated by direct calculation of distance from inferred and observed sequences, although the differences only approached borderline significance for K and were not significant for L and C (Table 3). Analysis based on MRCAs selected for the year 2 viral isolate clusters and the single plasma clone nearest each year 2 cluster gave comparable results (data not shown).

Both the summation of branch length method and the direct estimation of distances were based on results from phylogenetic reconstruction. As such, they reflect the accuracies and limitations of these methods (7, 16). In the case of analysis of branch lengths, the individual branch lengths given by fastDNAML were typically associated with fairly wide confidence intervals. The confidence intervals for the segments connecting the root of the year 2 viral isolate clusters and either the nearest plasma sequence (patients A, C, and M) or the root of plasma sequence clusters (B, K, and L) to the MRCA are shown in Table 4.

Correlation of evolutionary distance with residual replication represented by AUC$_{Net}$. Mean pairwise distances between plasma virus and virus isolated at year 2 (both corrected and uncorrected for intracompartment diversity) correlated with AUC$_{Net}$, with r^2 values of 0.55 and 0.6, respectively, but P values only approached statistical significance (0.09 and 0.067, respectively). However, differences in mean distance by analysis of branch lengths from MRCA to all virus isolates and to all plasma sequences from the same patient showed a significant correlation with AUC$_{Net}$: $r^2 = 0.889$ ($P = 0.0048$). Using a direct calculation from the inferred ancestral sequences, the r^2 value was 0.68 ($P = 0.043$) with AUC$_{Net}$ (Fig. 4). When MRCAs were selected based on all viral isolates but only the nearest plasma sequence(s) for each patient, similar correlations were noted (data not shown).

DISCUSSION

Latently infected resting T cells harboring replication-competent virus persist in treated patients despite the absence of detectable free virus in the blood (3, 9, 47). Whether this reservoir of virus is maintained as a result of a low level of ongoing viral replication or as a result of a slow decay rate carries important implications for the risk of development of drug resistance and treatment failure in such patients. This question is central to the success or failure of any eradication strategy based on currently available antiviral drugs.

By conventional measures, all subjects studied had excellent responses to therapy, with viral loads rapidly falling to below 200 copies/ml of serum or plasma upon initiation of antiviral

FIG. 3. Predicted protein sequences. All letter designations for amino acids (AA) conform to the standard International Union of Pure and Applied Chemistry code. The HXB2 reference sequence (Los Alamos National Laboratory) is given at the top with the region corresponding to the V3 loop marked by a heavy line and residues 306 and 322 identified with arrows. Subject and source are identified in the first column, with the consensus sequence in plasma at baseline given in its entirety (based on the most frequently occurring AA at each position, or when two AA occurred with equal frequency from the same source, the AA corresponding to the HXB2 reference at the same position). Shown next are clonal sequences from year 0 plasma, followed by the consensus sequence from the year 2 viral isolates and the clonal sequences from year 2 viral isolates. These sequences are shown with the following abbreviations in reference to the baseline plasma consensus sequence for the same patient: period, identity with the plasma consensus; dash, gap inserted to maintain alignment of all sequences shown; question mark, unresolved AA position; asterisk, nonsense mutation. Replacements are indicated by the appropriate code letter. The frequency with which a particular clonal sequence was encountered is shown in the first column adjacent to each sequence. For patient M, residues 306 and 322 have been boxed to highlight the substitutions noted.

TABLE 2. Pairwise genetic distances between baseline plasma virus and year 2 viral isolates[a]

Patient	Pairwise distance (uncorrected) (%)	Pairwise distance (Nei and Tajima correction) (%)
A	3.76	1.37
B	0.25	0.0005
L	2.0	0.92
K	3.54	3.18
C	3.46	1.51
M	7.19	4.96

[a] Pairwise genetic distances between sequences in plasma at time zero and viral isolates at 2 years. In increasing order, the uncorrected estimates of divergence are B ≪ L < C, K, A ≪ M. The corrected estimates are much more variable than the uncorrected estimates (coefficient of variation, 0.68 for the uncorrected estimates and 0.90 for the corrected estimates). In increasing order, the corrected estimates of divergence are B ≪ L, A, C < K < M.

therapy. These responses were sustained at levels below the threshold of detection of a more sensitive assay (<50 copies/ml) for periods approaching 2 years at the time virus was isolated (12, 13). Previous studies of these subjects had demonstrated the lack of development of new genotypic drug resistance over this period (47). However, a detailed examination of the serial HIV RNA levels in blood from these patients revealed varying patterns based on rapidity of decline of the viral load and in some cases on the intermittent reappearance of low-level viremia during the course of therapy. These qualitative differences were reflected quantitatively in the calculated AUC_{Net} values representing residual viremia from ongoing viral replication (and/or, to a small extent, from activation of latently infected cells in vivo [see Materials and Methods]). It is not known why the antiviral drug effect may vary among these patients in spite of identical therapies, similar prestudy drug treatment histories, and similar incidence of preexisting drug resistance (13, 46, 47). Such differences could be attributable to individual differences in drug absorption or drug metabolism or to variable adherence.

Pairwise genetic distances from year 2 viral isolates to corresponding baseline plasma virus and pairwise distances from year 2 viral isolates and baseline plasma virus to the ancestral sequence inferred from a maximum-likelihood phylogenetic reconstruction were examined to estimate viral evolution in these subjects. Use of simple pairwise distances from year 2 viral isolates to baseline plasma virus would be expected to be an accurate reflection of generations elapsed between time points if year 2 viral isolates were, in every case, descendent from the virus present in plasma at baseline. However, if viral isolates at year 2 arise from latently infected cells that might have been ancestral to those present in plasma at baseline or which might have descended independently from a common ancestor, simple pairwise distances and generations elapsed need not be directly proportional. So, while those three patients (C, K, and M) having the largest AUC_{Net} (e.g., those with slower initial decline of viremia and those with sporadic reappearance of viremia) had the highest mean pairwise distances and the three subjects (A, B, and L) with the lowest AUC_{Net} had the lowest pairwise distances, the correlation of these parameters failed to reach statistical significance.

To quantitatively analyze genetic relationships of virus isolated at year 2 and virus present in baseline plasma (time zero) without having to assume that year 2 virus descended directly from baseline plasma virus, we examined pairwise distances from each cloned sequence to the corresponding MRCAs. The approach of summing relevant branch segments benefits from

TABLE 3. Genetic distances to MRCAs[a]

Patient	Method	MRCA-to-base plasma virus distance ± SE (%)	No. of clones analyzed	MRCA-to-year 2 viral isolate ± SE (%)	No. of clones analyzed	Wilcoxon rank sum (P)	Difference mean branch lengths to MRCA
A	BL	4.194 ± 0.287	9	4.062 ± 0.273	10	0.667	−0.132
	DD	3.892 ± 0.226		4.210 ± 0.238		0.44	0.318
B	BL	0.233 ± 0.043	10	0.022 ± 0.037	13	0.0023	−0.21
	DD	0.232 ± 0.043		0.022 ± 0.037		0.0023	−0.21
C	BL	3.345 ± 0.427	9	5.491 ± 0.427	10	0.001	2.146
	DD	2.696 ± 0.164		2.731 ± 0.164		0.507	0.035
K	BL	1.67 ± 0.089	7	1.924 ± 0.074	10	0.0208	0.254
	DD	1.677 ± 0.092		1.912 ± 0.077		0.07	0.235
L	BL	2.16 ± 0.142	10	0.114 ± 0.135	10	0.0002	−2.046
	DD	1.67 ± 0.141		1.276 ± 0.134		0.112	−0.39
M	BL	2.72 ± 0.166	10	6.56 ± 0.198	7	0.0006	3.84
	DD	2.584 ± 0.272		5.251 ± 0.326		0.0006	2.67

[a] Genetic distances to MRCA from plasma-derived sequences and year 2 viral isolates by summation of branch lengths (BL) generated with fastDNAML (7, 30) or direct calculation from sequences (DD) generated with DNAML (PHYLIP 3.6) (7, 8). (The results shown are from analyses based on selection of an MRCA for all plasma and viral isolate sequences.) The standard error (SE) was computed with a pooled estimate of error variance. Wilcoxon rank sums compare values to MRCA from plasma virus with those from year two viral isolates. The difference of mean branch lengths to MRCA were computed by subtracting the mean plasma virus-to-MRCA branch lengths from the mean year 2 viral isolate-to-MRCA branch lengths.

the incorporation of the structure of the inferred phylogenies into the distance measurements but does not readily yield an appropriate confidence interval. Therefore, we have also reconstructed the MRCA sequences with a maximum-likelihood approach (implemented in PHYLIP version 3.6) (7, 8) and directly estimated evolutionary distance between these and the baseline (plasma) and year 2 (virus isolate) sequences. The estimates resulting from both of these approaches demonstrated significant correlations of differences in distance to the MRCA with AUC_{Net} (Fig. 4).

Findings consistent with sequence evolution in cultured virus from some patients but not from others could be explained by a sampling artifact (isolation of virus from few latently infected cells) or by a selection artifact from in vitro coculture conditions with some patients but not others (5, 23, 28). We have analyzed sequences of virus cultured at time zero from patient A (virus isolates from time zero were not available from the other patients). This baseline isolate clustered more closely with virus in plasma at time zero than with viral isolates from the year 2 time point (data not shown), indicating greater effects from the time of sampling than from in vitro culturing in this setting. Moreover, the strong correlation between sequence evolution (measured by pairwise distances to the MRCA) and residual replication inferred by the magnitude of AUC_{Net} supports in vivo biological differences over random sampling artifacts or artifacts from in vitro culture to explain

these differences. Additional studies of the nature of the sequence changes observed have been performed which show that in the cases of M and K, but not the other four subjects, the changes in fact reflect selective differences between year 0 and year 2 (11a).

In the case of patient M and possibly patient K, the intermittent appearance of detectable plasma viral RNA into the

TABLE 4. Confidence intervals[a]

Patient	MRCA to base plasma virus (%) (CI)	MRCA to year 2 viral isolate (%) (CI)
A	0.585 (0, 1.404)	0.293 (0, 0.872)
B	0.0 (0, 0.558)	0.0 (0, 0.558)
C	0 (0, 0.722)	0.583 (0, 1.399)
K	1.466 (0.154, 2.81)	1.78 (0.342, 3.257)
L	0.864 (0, 1.853)	0.0 (0, 0.590)
M	0.570 (0, 1.392)	2.727 (0.953, 4.561)

[a] Branch lengths with confidence intervals (CI) of segments joining the root of the plasma viral sequence(s) nearest the year 2 viral clusters with the MRCA (identified based on the nearest plasma clone[s] and all year 2 viral isolate sequences) (column 2) and joining the root of year 2 viral isolate clusters and the same MRCA (column 3). The data were generated with fastDNAML (7, 30) and correspond to the phylogenetic tree shown in Fig. 2.
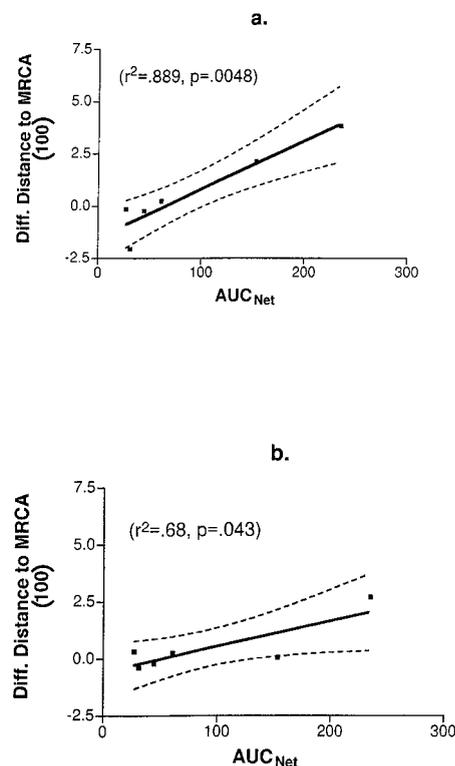
FIG. 4. Regression analysis of the AUC_{Net} and the differences in mean distances from plasma virus and virus isolates to the MRCA with inclusion of all plasma sequences calculated with summation of branch lengths (a) or by direct calculation of distance from sequences (b). The solid line represents the line of fit. The broken lines represent confidence curves for fit.

second year of therapy and the finding of evolution in the envelope sequences would be consistent with continuous or intermittent viral replication. Alternatively, but not mutually exclusively, in the case of patient M, where nonsynonymous substitutions in V3 were so frequent, sequences of year 2 viral isolates might reflect differences of a viral population maintained in an isolated anatomic compartment or a sanctuary site (20, 33, 48, 49). For patient C, reappearance of detectable free virus did not occur in the second year, although it was seen late into the first year, and the initial decline of plasma viremia was much more gradual than that seen for patient A, B, or L. In this case, the intermediate level of sequence evolution observed might be attributable either to viral replication occurring soon after initiation of therapy or to low levels of ongoing replication throughout the course of treatment.

Finally, in the cases of A, B, and L, treatment was associated with both the rapid decay of plasma virus levels and the sustained suppression of plasma viremia to undetectable levels. In these subjects, corrected pairwise genetic distances between sequences from baseline plasma and virus isolated later in therapy were smaller. In these three cases, mean distances from sequences of viral isolates at year 2 were equivalent to or even shorter than mean distances from baseline plasma to the MRCA, findings consistent with recovery of virus from cells infected at the time of or before the baseline plasma sequences. However, the failure to demonstrate sequence evolution for these patients in this particular viral reservoir does not rule out the possibility that very low levels of replication or replication in other compartments and in sanctuary sites not accessible to drug therapy persist.

These findings have several important implications for the understanding of HIV latency and the evaluation of antiviral therapies. First, they confirm that, in subjects who have sustained suppression of plasma viremia documented by the frequent application of the most sensitive assays (such as patients A, B, and L), a population of latently infected cells likely persists into the third year of therapy and that the maintenance of this reservoir of cells appears to be largely independent of discernible viral replication. From the available data, one would surmise that in such patients, the likelihood for emergence of drug resistance should be small. Second, even among patients who have apparent "suppression" of plasma viremia based on less sensitive assays (thresholds between 50 and 200 copies/ml), a subset will not have achieved complete suppression of viral replication. In these cases, the reservoir of replication-competent virus (whether in latently or productively infected cells) may in fact be replenished by continued viral propagation, a conclusion consistent with the demonstration of spliced RNA message and, in one case, changes seen in *pol* sequences in subjects previously studied (14).

Frequent testing for viremia with the most sensitive assays may permit the identification of such individuals with incomplete suppression of viral replication. The magnitude of risk for development of drug resistance under these circumstances is not known. Consequently, it is also not known whether, in the absence of demonstrable drug resistance, additions to or substitutions in antiviral regimens are warranted. However, these observations suggest that a less rapid initial decline in viral load and the sporadic reappearance of low levels of detectable viremia during therapy may signify incomplete suppression of viral replication and that such assessments may be meaningful in evaluating and comparing the potency of antiviral therapies, as has been proposed by others (44). Finally, these findings indicate that any measurement of the "clearance rate" of the reservoir of latently infected T cells can only be accurately performed on the very best characterized patients, employing,

at a minimum, both sensitive and frequent assays of residual RNA in blood to screen for incomplete suppression of viral replication.

ADDENDUM

Following the submission of our manuscript, Zhang et al. (50) reported the demonstration of viral replication in two of eight patients with primary HIV infection treated with antiviral therapy who had achieved undetectable plasma RNA levels. In the same issue, Furtado and colleagues (11b) reported the persistence of viral transcriptional activity in PBMC from treated, chronically infected patients with undetectable viral RNA, suggesting either ongoing replication or a transcriptionally active form of latent infection.

REFERENCES

1. **Adachi, A., H. E. Gendelman, S. Koenig, T. Folks, R. Willey, A. Rabson, and M. A. Martin.** 1986. Production of acquired immunodeficiency syndrome-associated retrovirus in human and nonhuman cells transfected with an infectious molecular clone. J. Virol. **59:**284–291.
1a. **Balfe, P., P. Simmonds, C. A. Ludlam, J. O. Bishop, and A. J. Leigh-Brown.** 1990. Concurrent evolution of human immunodeficiency virus type 1 in patients infected from the same source: rate of sequence change and low frequency of inactivating mutations. J. Virol. **64:**6221–6233.
2. **Cavert, W., D. W. Notermans, K. Staskus, S. Wietgrefe, M. Zupancic, K. Gebhard, K. Henry, Z. Q. Zhang, R. Mills, H. McDade, J. Goudsmit, S. A. Danner, and A. T. Haase.** 1997. Kinetics of response in lymphoid tissues to antiretroviral therapy of HIV-1 infection. Science **276:**960–964.
3. **Chun, T. W., L. Stuyver, S. B. Mizell, L. A. Ehler, J. M. Mican, M. Baseler, A. L. Lloyd, M. A. Nowak, and A. S. Fauci.** 1997. Presence of an inducible HIV latent reservoir during highly active antiretroviral therapy. Proc. Natl. Acad. Sci. USA **94:**13193–13197.
4. **De Jong, J.-J., J. Goudsmit, W. Keulen, B. Klaver, W. Krone, M. Tersmette, and A. de Ronde.** 1992. Human immunodeficiency virus type 1 clones chimeric for the envelope V3 domain differ in syncytium formation and replication capacity. J. Virol. **66:**757–765.
5. **Delassus, S., R. Cheynier, and S. Wain-Hobson.** 1991. Evolution of human immunodeficiency virus type 1 *nef* and long terminal repeat sequences over 4 years in vivo and in vitro. J. Virol. **65:**225–231.
6. **Delwart, E. L., P. Heng, H. W. Sheppard, D. Wolpert, A. U. Neumann, B. Korber, and J. I. Mullins.** 1997. Slower evolution of human immunodeficiency virus type 1 quasispecies during progression to AIDS. J. Virol. **71:**7498–7508.
7. **Felsenstein, J.** 1993. Phylogenetic inference package (Phylip) 3.5. University of Washington, Seattle.
8. **Felsenstein, J.** Personal communication.
9. **Finzi, D., M. Hermankova, T. Pierson, L. Carruth, C. Buck, R. Chaisson, T. Quinn, K. Chadwick, J. Margolick, R. Brookmeyer, J. Gallant, M. Markowitz, D. D. Ho, D. Richman, and R. Siliciano.** 1997. Identification of a reservoir for HIV in patients on highly active antiretroviral therapy. Science **278:**1295–1300.
10. **Finzi, D., J. Blankson, J. D. Siliciano, J. B. Margolick, K. Chadwick, T. Pierson, K. Smith, J. Lisziewicz, F. Lori, C. Flexner, T. C. Quinn, R. E. Chaisson, E. Rosenberg, B. Walker, S. Gange, J. Gallant, and R. F. Siliciano.** 1999. Latent infection of CD4 T cells provides a mechanism for lifelong

persistence of HIV-1, even in patients on effective combination therapy. Nat. Med. **5:**512–517.

11. **Fouchier, R. A. M., M. Groenink, N. A. Kootstra, M. Tersmette, H. G. Huisman, F. Miedema, and H. Schuitemaker.** 1992. Phenotype-associated sequence variation in the third variable domain of the human immunodeficiency virus type 1 gp120 molecule. J. Virol. **66:**3183–3187.

11a. **Frost, S. D. W., et al.** Unpublished data.

11b. **Furtado, M. R., D. S. Callaway, J. P. Phair, K. Kunstman, J. L. Stanton, C. A. Macken, A. S. Perelson, and S. M. Wolinsky.** 1999. Persistence of HIV-1 transcription in peripheral blood mononuclear cells in patients receiving potent antiretroviral therapy. N. Engl. J. Med. **340:**1614–1622.

12. **Gulick, R., J. W. Mellors, D. Havlir, J. Eron, C. Gonzalez, D. McMahon, L. Jonas, A. Meibohm, D. Holder, W. A. Schleif, J. H. Condra, E. Emini, R. Isaacs, J. Chodakewitz, and D. Richman.** 1998. Simultaneous vs. sequential initiation of therapy with indinavir, zidovudine, and lamivudine for HIV-1 infection: 100 week follow-up. JAMA **280:**35–41.

13. **Gulick, R. M., J. W. Mellors, D. Havlir, J. J. Eron, C. Gonzalez, D. McMahon, D. D. Richman, F. T. Valentine, P. Deutsch, A. Meibohm, D. Holder, W. A. Schleif, J. H. Condra, E. A. Emini, and J. A. Chodakewitz.** 1997. Treatment with a combination of indinavir, zidovudine and lamivudine in HIV-infected adults with prior antiretroviral use. N. Engl. J. Med. **337:**734–739.

14. **Günthard, H. F., J. K. Wong, C. C. Ignacio, J. C. Guatelli, N. L. Riggs, D. Havlir, and D. D. Richman.** 1998. Human immunodeficiency virus replication and genotypic resistance in blood and lymph nodes after a year of potent antiretroviral therapy. J. Virol. **72:**2422–2428.

15. **Hahn, B. H., G. M. Shaw, M. E. Taylor, R. R. Redfield, P. D. Markham, S. Z. Salahuddin, F. Wong-Staal, R. C. Gallo, E. S. Parks, and W. P. Parks.** 1986. Genetic variation in HTLV-III/LAV over time in patients with AIDS or at risk for AIDS. Science **232:**1548–1553.

16. **Hillis, D., J. Huelsenbeck, and C. Cunningham.** 1994. Application and accuracy of molecular phylogenies. Science **264:**671–675.

17. **Hudson, R. R.** 1990. Gene genealogies and the coalescent process, p. 1–44. *In* D. Futuyma and J. Antonovics (ed.), Oxford surveys in evolutionary biology. Oxford University Press, Oxford, United Kingdom.

18. **Kingman, J. F. C.** 1982. On the genealogy of large populations, p. 27–43. *In* J. Gani and E. J. Hannan (ed.), Applied probability trust. Sheffield, England.

19. **Korber, B. T., E. E. Allen, A. D. Farmer, and G. Myers.** 1995. Heterogeneity of HIV-1 and HIV-2. AIDS **9**(Suppl. A):S5–S18.

20. **Korber, B. T. M., K. J. Kunstman, B. K. Patterson, M. Furtado, M. M. McEvilly, R. Levy, and S. M. Wolinsky.** 1994. Genetic differences between blood- and brain-derived viral sequences from human immunodeficiency virus type 1-infected patients: evidence of conserved elements in the V3 region of the envelope protein of brain-derived sequences. J. Virol. **68:**7467–7481.

21. **Korber, B. T. M., K. MacInnes, R. F. Smith, and G. Myers.** 1994. Mutational trends in V3 loop protein sequences observed in different genetic lineages of human immunodeficiency virus type 1. J. Virol. **68:**6730–6744.

22. **Kuiken, C., G. Zwart, E. Baan, R. Coutinho, J. van den Hoek, and J. Goudsmit.** 1993. Increasing antigenic and genetic diversity of the V3 variable domain of the HIV-1 envelope protein in the course of the AIDS epidemic. Proc. Natl. Acad. Sci. USA **90:**9061–9065.

23. **Kusumi, K., B. Conway, S. Cunningham, A. Berson, C. Evans, A. K. N. Iversen, D. Colvin, M. V. Gallo, S. Coutre, E. G. Shpaer, D. V. Faulkner, A. deRonde, S. Volkman, C. Williams, M. S. Hirsch, and J. I. Mullins.** 1992. Human immunodeficiency virus type 1 envelope gene structure and diversity in vivo and after cocultivation in vitro. J. Virol. **66:**875–885.

24. **Learn, G. H., B. T. Korber, B. Foley, B. Hahn, S. M. Wolinsky, and J. I. Mullins.** 1996. Maintaining the integrity of the HIV sequence databases. J. Virol. **70:**5720–5730.

25. **Leitner, T., D. Escanilla, C. Franzen, M. Uhlen, and J. Albert.** 1996. Accurate reconstruction of a known HIV-1 transmission history by phylogenetic tree analysis. Proc. Natl. Acad. Sci. USA **93:**10864–10869.

26. **Leitner, T., S. Kumar, and J. Albert.** 1997. Tempo and mode of nucleotide substitutions in *gag* and *env* gene fragments in human immunodeficiency virus type 1 populations with known transmission history. J. Virol. **71:**4761–4770.

27. **Lukashov, V. V., C. Kuiken, D. Vlahov, R. Coutinho, and J. Goudsmit.** 1996. Evidence for HIV-1 strains of U.S. intravenous drug users as founders of AIDS epidemic among intravenous drug users in northern Europe. AIDS Res. Hum. Retroviruses **12:**1179–1183.

28. **Michael, N. L., G. Chang, P. K. Ehrenberg, M. T. Vahey, and R. R. Redfield.** 1993. HIV-1 proviral genotypes from the peripheral blood mononuclear cells of an infected patient are differentially represented in expressed sequences. J. AIDS **6:**1073–1085.

29. **Nei, M., and L. Jin.** 1989. Variances of the average numbers of nucleotide substitutions within and between populations. Mol. Biol. Evol. **6:**290–300.

30. **Olsen, G. J., H. Matsuda, R. Hagstrom, and R. Overbeek.** 1994. FastDNAML 1.0. University of Illinois, Urbana, and Argonne National Laboratory, Argonne, Ill.

30a. **Page, R. D. M.** 1996. Treeview: and application to display phylogenetic trees on personal computers. Comput. Appl. Biosci. **12:**357–358.

31. **Perelson, A. S., P. Essunger, Y. Cao, M. Vesanen, A. Hurley, K. Saksela, M. Markowitz, and D. D. Ho.** 1997. Decay characteristics of HIV-1 infected compartments during combination therapy. Nature **387:**188–191.

32. **Perelson, A. S., A. U. Neumann, M. Markowitz, J. M. Leonard, and D. D. Ho.** 1996. HIV-1 dynamics in vivo: virion clearance rate, infected cell lifetime, and viral generation time. Science **271:**1582–1586.

33. **Power, C., J. C. McArthur, R. T. Johnson, D. E. Griffin, J. D. Glass, S. Perryman, and B. Chesebro.** 1994. Demented and nondemented patients with AIDS differ in brain-derived human immunodeficiency virus type 1 envelope sequences. J. Virol. **68:**4643–4649.

34. **Richman, D. D., and S. A. Bozzette.** 1994. The impact of syncytium-inducing phenotype of human immunodeficiency virus on disease progression. J. Infect. Dis. **169:**968–974.

35. **Rodrigo, A.** 1998. Coalescent approaches to HIV population genetics, p. 54. *In* Proceedings of the 5th Annual HIV Dynamics and Evolution Conference.

36. **Saag, M. S., B. H. Hahn, J. Gibbons, Y. Li, E. S. Parks, W. P. Parks, and G. M. Shaw.** 1988. Extensive variation of human immunodeficiency virus type-1 in vivo. Nature **334:**440–444.

37. **Shankarappa, R., P. Gupta, G. Learn, A. Rodrigo, C. R. Rinaldo, Jr., M. C. Gorry, J. I. Mullins, P. L. Nara, and G. D. Ehrlich.** 1998. Evolution of HIV-1 envelope sequences in infected individuals with differing disease progression profiles. Virology **241:**251–259.

38. **Simmonds, P., P. Balfe, C. A. Ludlam, J. O. Bishop, and A. J. Leigh-Brown.** 1990. Analysis of sequence diversity in hypervariable regions of the external glycoprotein of human immunodeficiency virus type 1. J. Virol. **64:**5840–5850.

39. **Simmonds, P., L. Q. Zhang, F. McOmish, P. Balfe, C. A. Ludlam, and A. J. Leigh-Brown.** 1991. Discontinuous sequence change of human immunodeficiency virus (HIV) type 1 *env* sequences in plasma viral and lymphocyte-associated proviral populations in vivo: implications for models of HIV pathogenesis. J. Virol. **65:**6266–6276.

40. **Speck, R. F., K. Wehrly, E. J. Platt, R. E. Atchison, I. F. Charo, D. Kabat, B. Chesebro, and M. A. Goldsmith.** 1997. Selective employment of chemokine receptors as human immunodeficiency virus type 1 coreceptors determined by individual amino acids in the envelope V3 loop. J. Virol. **71:**7136–7139.

41. **Tajima, F.** 1983. Evolutionary relationship of DNA sequences in finite populations. Genetics **105:**437–460.

42. **van't Wout, A., L. Ran, C. Kuiken, N. Kootstra, S. Pals, and H. Schuitemaker.** 1998. Analysis of the temporal relationship between human immunodeficiency virus type 1 quasispecies in sequential blood samples and various organs obtained at autopsy. J. Virol. **72:**488–496.

43. **Wainberg, M. A., W. C. Drosopoulous, H. Salomon, M. Hsu, G. Borkow, M. Parniak, Z. Gu, Q. Song, J. Manne, and S. Islam.** 1996. Enhanced fidelity of 3TC-selected mutant HIV-1 reverse transcriptase. Science **271:**1282–1285.

44. **Weverling, G. J., J. M. A. Lange, S. Jurriaans, J. M. Prins, V. Lukashov, D. W. Notermans, M. Roos, H. Schuitemaker, R. M. W. Hoetelmans, S. V. Danner, J. Goudsmit, and F. de Wolf.** 1998. Alternative multidrug regimen provides improved suppression of HIV-1 replication over triple therapy. AIDS **12:**F117–F122.

45. **Wolinsky, S. M., B. T. Korber, A. U. Neumann, M. Daniels, K. J. Kuntsman, A. J. Whetsell, M. R. Furtado, Y. Cao, D. D. Ho, J. T. Safrit, et al.** 1996. Adaptive evolution of human immunodeficiency virus-type 1 during the natural course of infection. Science **272:**537–542.

46. **Wong, J. K., H. F. Gunthard, D. V. Havlir, Z. Q. Zhang, A. T. Haase, C. C. Ignacio, S. Kwok, E. A. Emini, and D. D. Richman.** 1997. Reduction of HIV-1 in blood and lymph nodes following potent anti-retroviral therapy and the virologic correlates of treatment failure. Proc. Natl. Acad. Sci. USA **94:**12574–12579.

47. **Wong, J. K., M. Hezareh, H. F. Gunthard, D. Havlir, C. C. Ignacio, C. Spina, and D. D. Richman.** 1997. Recovery of replication competent HIV despite prolonged suppression of plasma viremia. Science **278:**1291–1295.

48. **Wong, J. K., C. C. Ignacio, F. Torriani, D. Havlir, N. J. S. Fitch, and D. D. Richman.** 1997. *In vivo* compartmentalization of HIV: evidence from the examination of *pol* sequences from autopsy tissues. J. Virol. **70:**2059–2071.

49. **Zhang, H., G. Dornadula, M. Beumont, L. Livornese, Jr., B. Van Uitert, K. Henning, and R. J. Pomerantz.** 1998. Human Immunodeficiency Virus type 1 in the semen of men receiving highly active antiretroviral therapy. N. Engl. J. Med. **339:**1803–1809.

50. **Zhang, L., B. Ramratnam, K. Tenner-Racz, Y. He, M. Vesanen, S. Lewin, A. Talal, P. Racz, A. S. Perelson, B. T. Korber, M. Markowitz, and D. D. Ho.** 1999. Quantifying residual HIV-1 replication in patients receiving combination antiretroviral therapy. N. Engl. J. Med. **340:**1605–1613.